Dye Removal Probing by Electrocoagulation Process:
Modeling by MLR and ANN Methods

[1]AFSHIN MALEKI, [1]HIUA DARAEI*, [2]LOGHMAN ALAEI, [1]LEILA ABASI AND [1]ANISE IZADI
[1]*Kurdistan Environmental Health Research Center, Kurdistan,*
University of Medical Sciences, Sanandaj, Iran.
[2]*Institute of Biochemistry and Biophysics, University of Tehran, Tehran, Iran.*
hiua.Daraei@muk.ac.ir*

Summary. The present study performed to investigate dye removal efficiency (DR%) of solutions containing direct blue 71 (DB71) using electrocoagulation (EC) process. applied voltage (V_{EC}), Initial pH of the solution (PH_0), time of electrolysis (t_{EC}) and initial dye concentration (C_0) considered as more effective operational parameters. The experimental data obtained in a laboratory batch reactor. The achieved DR% of 4.4-99.3 gained under experimental conditions. The multiple linear regression (MLR) and non linear artificial neural network (ANN) models utilized to EC modeling and DR% predicting. By applying best MLR and ANN models to predict the test set, Q^2_{ext} and RMSE determined 0.79 and 13.7 for MLR and 0.93 and 8.01 for ANN. Further tests and data treatments were done for more validation and introduce model applications and also to clarify other aspects of EC, such as Leave-n-Out (n=1, 43-44, 74) cross-validation, energy consumption calculation, graphical prediction of the optimum experimental conditions and diversity test. The experimental results proved that EC is an effective way to treat dye solutions containing DB71. V_{EC}, pH_0, t_{EC} and C_0 parameters influenced DR% and the ANN and MLR have been successfully used to modeling EC.

Keywords: Dye removal; Direct Blue71; Electrocoagulation; Multiple linear regression; artificial neural networks.

Introduction

Dyes in wastewaters are a serious environmental concern. They can absorb and reflect sunlight and prevent it from reaching the microorganisms of water. Thus, bacteria have not suitable circumstances to grow. This leads to disastrous effects on food chain [1, 2]. Dyes are classified by their chemical and dyeing properties. The main groups are azo, anthraquinone, phthalocyanine and triarylmethane [3]. Synthetic azo dyes comprise more than half of all dyes production [4]. They are used in textiles, foodstuffs, leather and many other products. Also, azo dyes are about half of dyes used in textile industry. Because of their toxicity, a lot of problems have arisen due to release of some of these products into the environment[3, 5].

Some methods have been introduced to remove dyes from colored effluents such as adsorption, precipitation, chemical degradation, photodegradation, biodegradation, chemical coagulation and electrocoagulation. Owing to the complex structures of azo dyes, biological, physical and chemical treatments of dye effluents are inefficient [6-8]. In the other hand, azo dyes are usually designed to resist against aerobic biodegradation [4]. Adsorption and precipitation processes are relatively time-consuming and expensive with low efficiency [9]. Chemical degradation by oxidative agents such as chlorine is the most important and effective method, but it produces some high toxic side products such as organochlorine compounds. Photo oxidation by UV/H_2O_2 or UV/TiO_2 needs additional chemicals and therefore causes secondary pollution [6, 7].

In recent years, electrochemical treatment methods such as electro-oxidation and electrocoagulation (EC) have drawn great attention as a Biocompatible and cost-effective technique. EC involves the in-situ generation of coagulants by electrolytic oxidation of an appropriate sacrificial anode. The electrical current causes the dissolution of metal electrodes into wastewater. The metal ions, at an appropriate pH, can form wide ranges of coagulated species and metal hydroxides which destabilize and aggregate the suspended particles or precipitates and adsorb dissolved contaminants [10].

The electrodes can be made of aluminum (Al) or iron (Fe) plates or from scraps such as Fe or Al millings, cuttings, etc. The Al plates have applied in water and wastewater treatment either alone or in combination with Fe plates due to the high coagulation efficiency of Al^{3+} ion [11]. The electrolytic dissolution of the Al anode produces the cationic monomeric species such as Al^{3+} and Al

---

$(OH)_2^+$ in acidic solutions. In appropriate pH values, they transform first to $Al(OH)_3$ and finally polymerize to $Al_n(OH)_{3n}$ based on following equations :

$$Al \rightarrow Al^{3+}(aq)+3e^-$$
$$Al^{3+}(aq)+3H_2O \rightarrow Al(OH)_3+3H^+(aq)$$
$$nAl(OH)_3 \rightarrow Al_n(OH)_{3n}$$
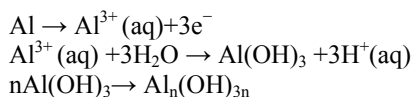
However, depending on the pH of the aqueous medium, other ionic species, such as $Al(OH)_2^+$, $Al_2(OH)_2^{4+}$ and $Al(OH)_4^-$ may also be produced in the system. In addition, various forms of charged multimeric hydroxo Al^{3+} species may be appear under given conditions. These gelatinous charged hydroxo cationic complexes can effectively remove pollutants via adsorption [12].

EC has been successfully used for decades to treat the wastewaters of various sources like: textile [10, 13], food and protein [14], phosphate [15], yeast [16], urban [17], saline [18], chemical fiber plant [19], restaurants [14], tar sand and oil shale [20], landfill leachate [21], arsenic containing smelter [22] and dye stuff [23]. Although there have been a remarkable amount of studies on EC technique for wastewater treatment, but large-scale applications of this technology have been relatively few. One possible reason is the energy demand of the EC. The aspect of hydrogen recovery from the EC has been studied and can be a probable solution for the inefficiency of EC [24].

Appearance of new methods like artificial neural network for EC modeling reported recently [7, 25-29]. The reports cannot be confident without more rigorous statistical validations. Applications of EC to remove the azo dyes and use of ANN method to model the EC have inspired us to perform more exhaustive studies. The DR% of the dye solution containing DB71 azo dye has been investigated by EC method. The dye is soluble in water and belongs to Azo dyes group. Several parameters such as EC voltage (V_{EC}), initial pH (pH_0), initial concentration (C_0) and EC time (t_{EC}) were investigated and obtained data used to construct the multiple linear regression (MLR) and artificial neural network (ANN) models to predict DR% of EC [30-32].

Results and discussion

DR%

In the first three concentrations of DB71, DR% measured in different levels of PH_0, V_{EC} and t_{ec}. The levels of each parameter selected based on our best information of previous studies and also regarded to actual conditions of textile wastewaters.

The obtained results summarized graphically in Fig. 1. A Glance at Fig. 1 shows two levels for DR%, more than 80% (green dots) and less than 80% (blue dots). Fig. 2 displays the effect of each investigated parameters. As it seen from Fig. 2, different levels of experimental parameters cause to different DR% and various rates of dye removal.

Fig. 2 also shows that the removal rate before achieving 'level off' of DR% diagram follows two different patterns, slow and fast. Two lines with different slopes on either side about DR% 50 (inversion point) in diagrams of Fig. 2 obviously demonstrate this fact. In order to more explanation, competition between two different mechanisms before and after inversion point suggested. First, coagulant products and dye adsorb to form small new coagulum particles. The second suggested mechanism is dye adsorption on the formed coagula in the first mechanism. We assume that the significance of second mechanism increases when the first mechanism proceeds enough. Refer to results; the importance of second mechanism is more than first one near about DR% 50. It explains the further speed of removal after inversion points in diagrams.

Effect of C_0 and t_{EC} on DR%

Actually, the textile plant's wastewaters vary in dye concentration. So it is essential to investigate the effect of C_0 on EC. Therefore, different dye concentrations at three levels 20, 50 and 100 (mg/L) studied. Fig. 2 shows that, solutions containing higher C_0 need more t_{EC} to reach higher level of DR% (> 80). The reverse dependence of DR% to C_0 presented with a histogram in Fig. 3 by a different way.

As seen from the histogram in Fig. 3, in all three concentrations, 72 samples provided with similar conditions. When C_0 was 20 (mg/L) only 28 samples didn't achieve the higher level of DR% but, when C_0 was 100 (mg/L) the value raised to 40. It is necessary to be mentioned that this pattern of dependence has been reported previously [7]. It is based on this fact; more initial concentration of dye requires more coagulants (Al^{3+}) to remove. The electro coagulant concentration is dependent on applied voltage, conductivity of solutions, PH_0 and t_{EC}. When PH_0, V_{EC}, and C_0 are constant, t_{EC} is the only factor that plays an effective role on production of coagulant and then DR%. Therefore, higher C_0 requires more coagulant to remove and more coagulant requires more t_{EC} to produce. In Fig. 2 we illustrated this fact that t_{ec} affected DR%. Actually, by increasing t_{ec} level of PH_0, V_{EC} and C_0 also increased, which finally led to DR% growth.
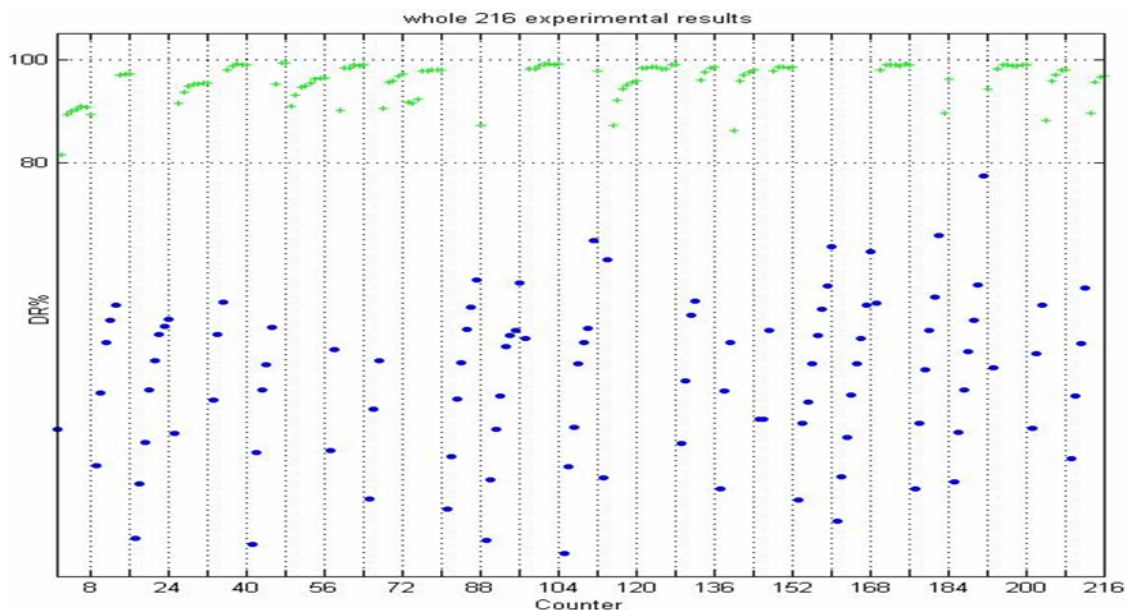
Fig. 1:   DR% in 216 samples and 27 experiments.

Effect of pH$_0$ on DR%

Experiments were performed by adjusting the pH$_0$ at 4, 7 and 9 to investigate the effect of pH$_0$ on DR%. Effects of pH$_0$ on EC are shown in Fig. 2 and 4. Conditions with pH 4 had the best efficiency in all tests. In the other hand, DR% >80 and t$_{EC}$< 30 min at the same time were available at PH$_0$ 4, only (Fig. 2). The results were in good agreement with well-known statement that the influent pH is a significant parameter influencing the performance of EC [33].

The solid precipitate of aluminum hydroxide is formed in pH 4-6. solubility of aluminum hydroxide increases when the solution becomes either more acidic or alkali .

$Al(OH)_3 + OH^- \rightarrow Al(OH)_4^-$
$Al(OH)_3 + H^+(aq) \rightarrow Al(OH)_2^+(aq) + H_2O$
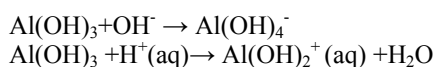
It is in good agreement with optimum value for pH$_0$ 4 in our experiments. But about pH$_0$ 7, that is near the optimum range, we can say, the prominence of pH 4 rather than 7 is due to effect of pH on the other parameters like solution conductivity and I$_{EC}$.

Effect of V$_{EC}$ on DR%

V$_{EC}$ is an important factor strongly influences the performance of EC [34]. Fig. 2 proves the direct relation between DR% and V$_{EC}$ in our experiments. In the other hand, DR% achieved higher value in less t$_{ec}$ for similar combined conditions of pH$_0$ and C$_0$ when V$_{EC}$ is in the higher level.

Furthermore, Fig. 5 shows the effect of V$_{EC}$ in a different manner. It shows that the number of experiments achieved DR% upper 80 will increase when V$_{EC}$ increases, too. W.L. Chou *et.al*, reported that lower voltage was unable to completely destabilize the suspended oxide particles in the solution [34]. Also, it may be due to V$_{EC}$ that causes more I$_{EC}$ which finally results in more coagulant production.

Results of ANN model

The best ANN model constructed using two hidden layers, 14 neurons for both hidden layers and 0.11 learning rate. The tansig transfer function selected for input and hidden layers and purelin for output. Once the network trained, the weights and bias of each neuron and layer are saved in the ANN model. Then, they are used to estimate the test set. The (4:14:14:1) ANN trained with 130 dataset by the back propagation algorithm. The tansig and purelin transfer functions define as Equations 1 and 2, respectively. In order to evaluate the ANN model predictability, the sample of ANN model predictions and their related experimental results are shown together as colored surface and black dots, respectively (Fig. 6).

$$a = \text{tansig(n)} \quad = \frac{2}{(1 + \exp(-2n))} - 1 \qquad (1)$$

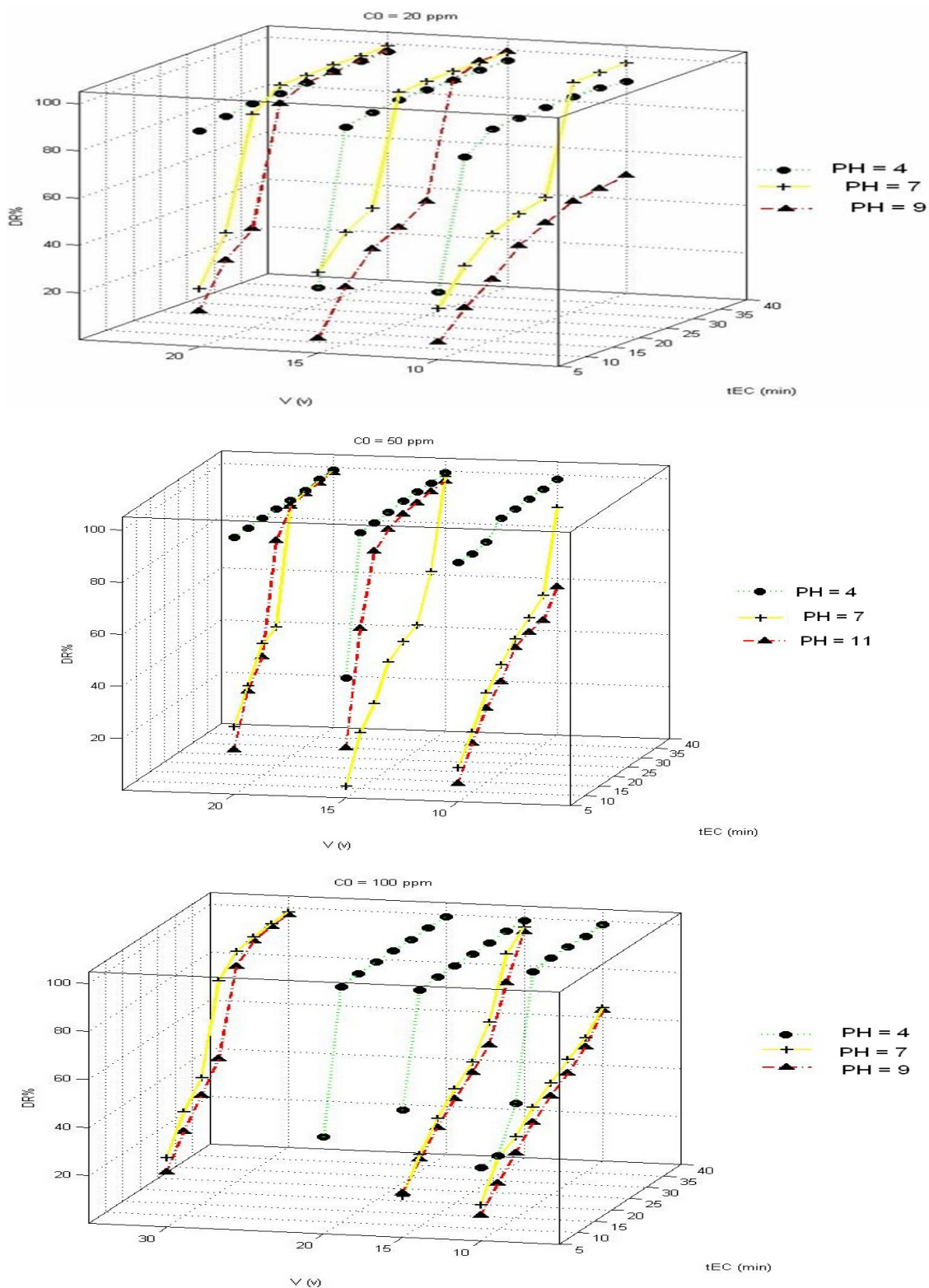$$a = \text{purelin} \quad (n) = n \qquad \textbf{(2)}$$
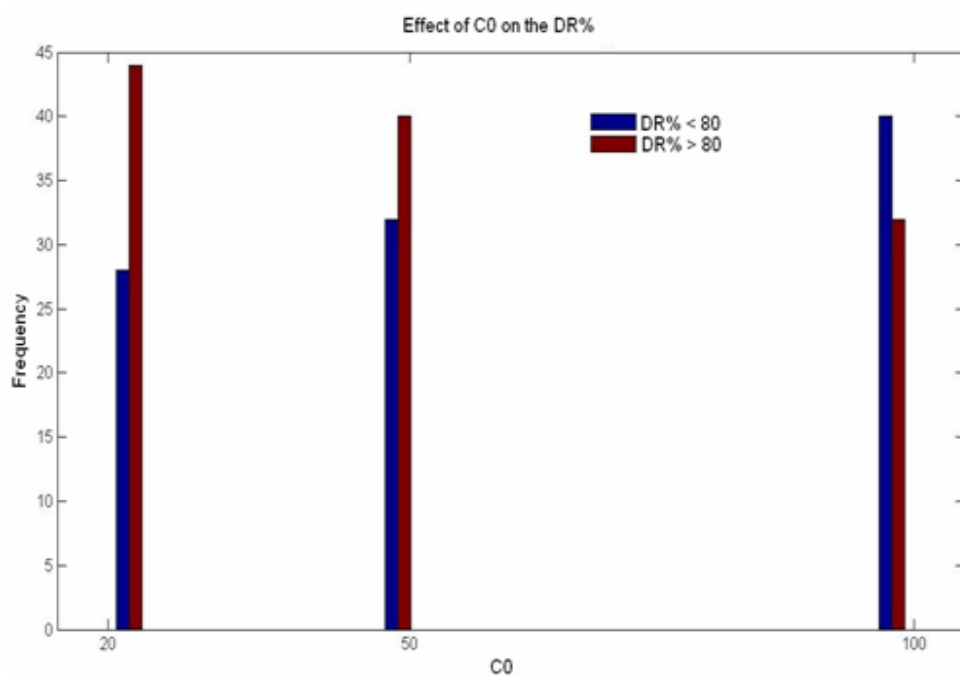
Fig. 2:   The DR% of all 27 experiments.

Fig. 3:   Histogram of two DR% level (red lines: less than 80% and blue lines: more than 80%) for the three investigated levels of C_0.
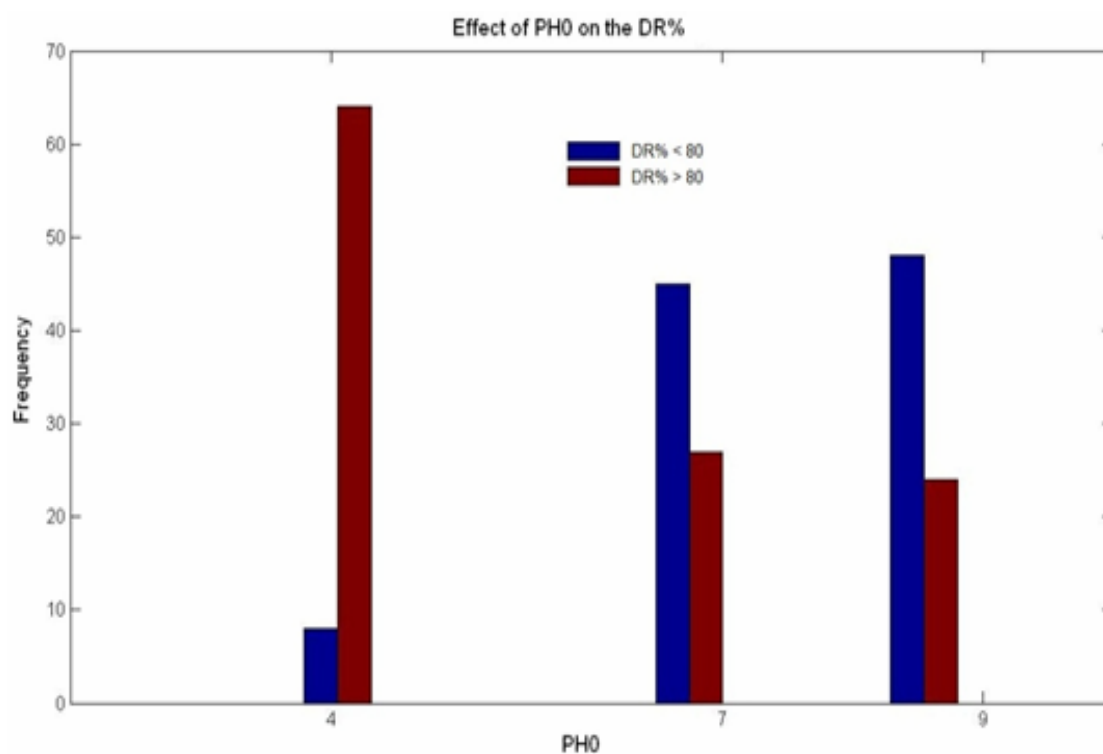

Fig. 4:   Histogram of two DR% levels (red line: less than 80% and blue line: more than 80%) for the three studied pH_0 levels.
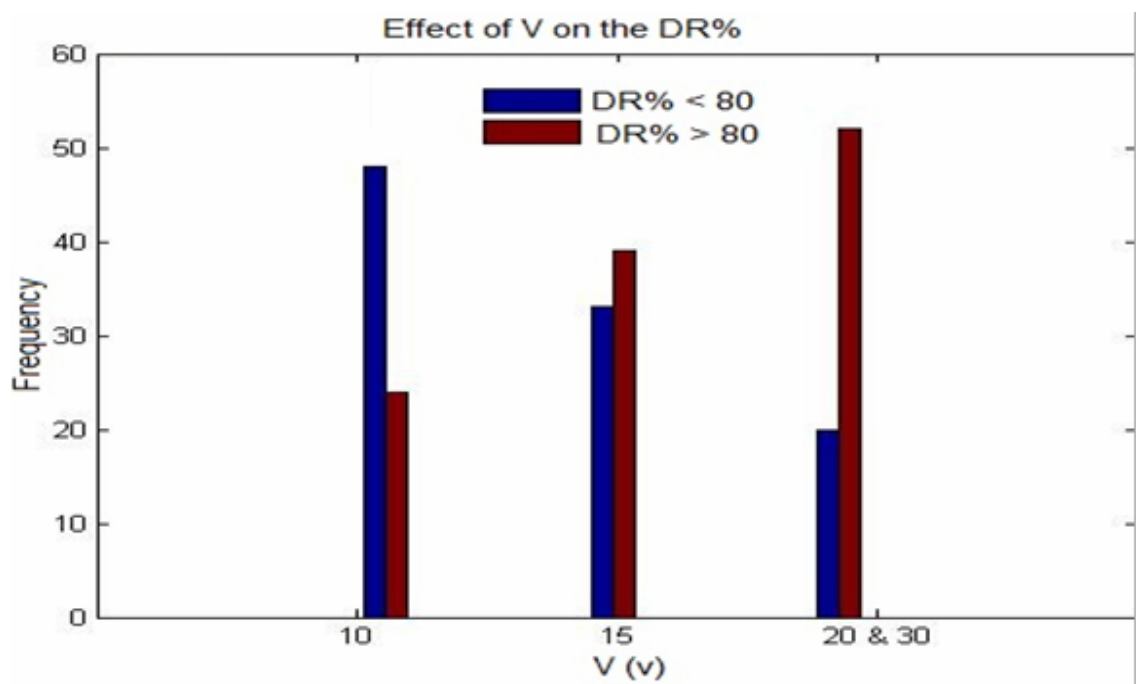
Fig. 5:   Histogram of two DR% levels (red line: less than 80% and blue line: more than 80%) for three studied
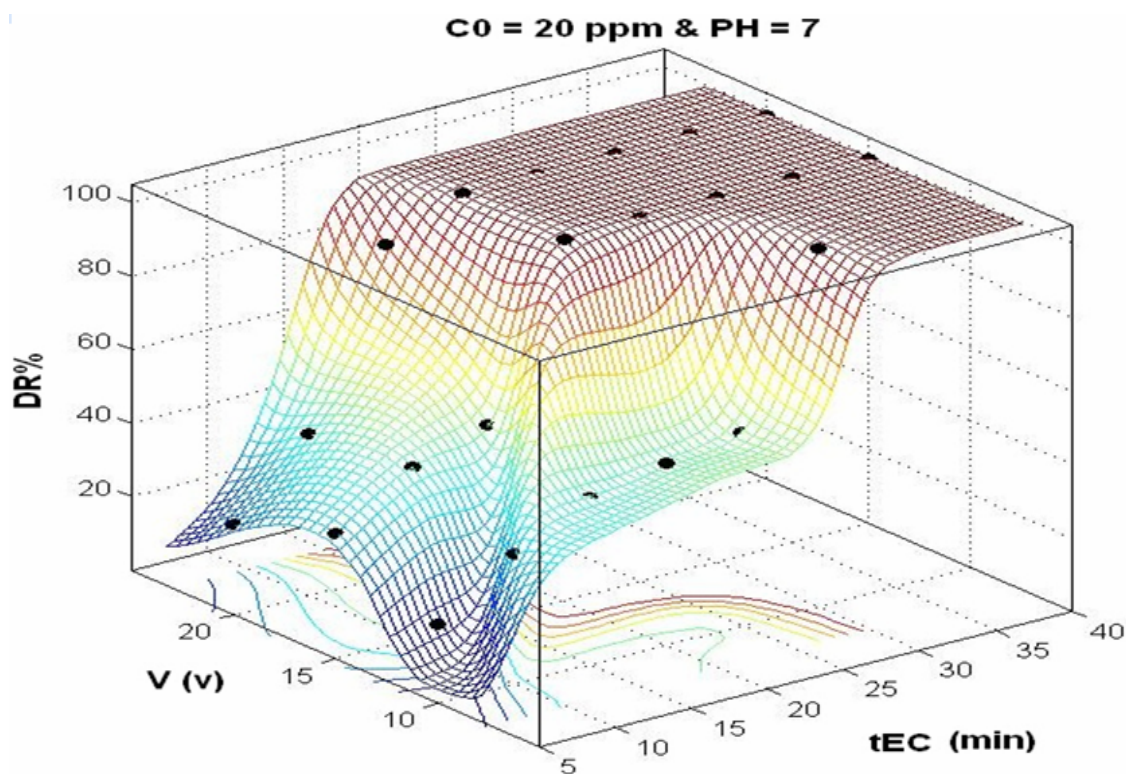V$_{EC}$ levels..

Fig. 6:   Plots of the ANN predicted values (colored surface) versus experimental DR% values (black dots) for
C$_0$ = 20 (mg/L) and pH$_0$ = 7.

Results of MLR

In order to compare ANN model with a simple classic approach, The SMLR method applied to develop a new model based on same train set of ANN. To improve the MLR model, 10 additional quadratic interaction effects considered rather than only 4 variables used in ANN model. For preventing co-linearity effect, the number of inputs reduced from 14 to 9 using SMLR algorithm [35-37]. The best obtained model based on SMLR algorithm presented by Equation 3.

$DR\% = 113.65 - 0.104\ (C_0) + 4.02\ (V_{EC}) - 31.82\ (PH_0) + 2.3\ (t_{EC}) + 0.3\ (V_{EC})(PH_0) + 0.245\ (PH_0)\ (t_{EC}) - 0.051\ (t_{EC})^2 - 0.125\ (V_{EC})^2 + 1.19\ (PH_0)^2$ (3)

The statistical parameters of the new nine models are listed in Table-1. The sample of MLR prediction values of DR% are presented graphically in Fig. 7 in the same way done for ANN model.

Comparison between ANN and MLR models

ANN and MLR models have been compared regarding their predictability. The plots of predicted versus experimental DR% for MLR and ANN models are presented in Fig. 8 and 9. A summary of statistical comparisons of ANN and MLR are given in Table-2. Based on above mentioned results and other reports, it appears that the ANN model described here is superior for predicting DR%.

Graphical Prediction of Optimum Conditions

Forecasting the optimum range of operational parameters to reduce the cost and fallacy of experiments is final aim of each experimental modeling system. In this study, graphical method of optimum parameters selected which has been declared based on MLR and ANN models prediction. Therefore, the new optimum experimental condition obtained using graphical method, tested in laboratory and the obtained DR% compared with MLR and ANN model predictions. It is also the additional test for MLR and ANN comparison. On the other hand, each real sample of textile dye wastewater has its own C_0 and pH_0. Then it is very important to obtain the best DR% for new condition regarding optimum t_{EC} and V_{EC}.

Therefore, a sample of DB71 solution with $C_0 = 35$ (mg/L) prepared and its pH_0 adjusted to 6.7. In the following, two diagrams are presented based on MLR and ANN models prediction in Fig. 10. As the diagrams show, two models have an obvious difference in prediction. The ANN model predicts the efficient condition with optimum t_{EC} about 20 (min) and 17 (v) and DR% more than 94 for this condition; however the MLR model predicts the DR% less than 80 for the same condition. The experimental results can be used to compare the predictability of the two models. The experimental, DR% was 97.21, that is in good agreement with ANN results. It is also additional evidence to ANN prominence.

Table-1: Nine descriptor statistical parameters.

	Const.	C_0	V	PH_0	t_{EC}	$(PH_0)(t_{EC})$	t_{EC}^2	PH^2	V^2	$(V)(PH_0)$
Coeff.	113.65	-0.104	4.02	-31.82	2.30	0.245	-0.051	1.19	-0.125	0.30
t.value	-	-2.52	2.84	-5.02	3.77	4.47	-4.47	2.53	-3.11	1.99
p.value	-	0.013	0.005	0.000	0.000	0.000	0.000	0.013	0.002	0.048

Where b_i, st. error and t-test are the regression coefficients, standard errors of the regression coefficients and t significance respectively.

Table 2. The statistical comparisons of ANN and MLR models

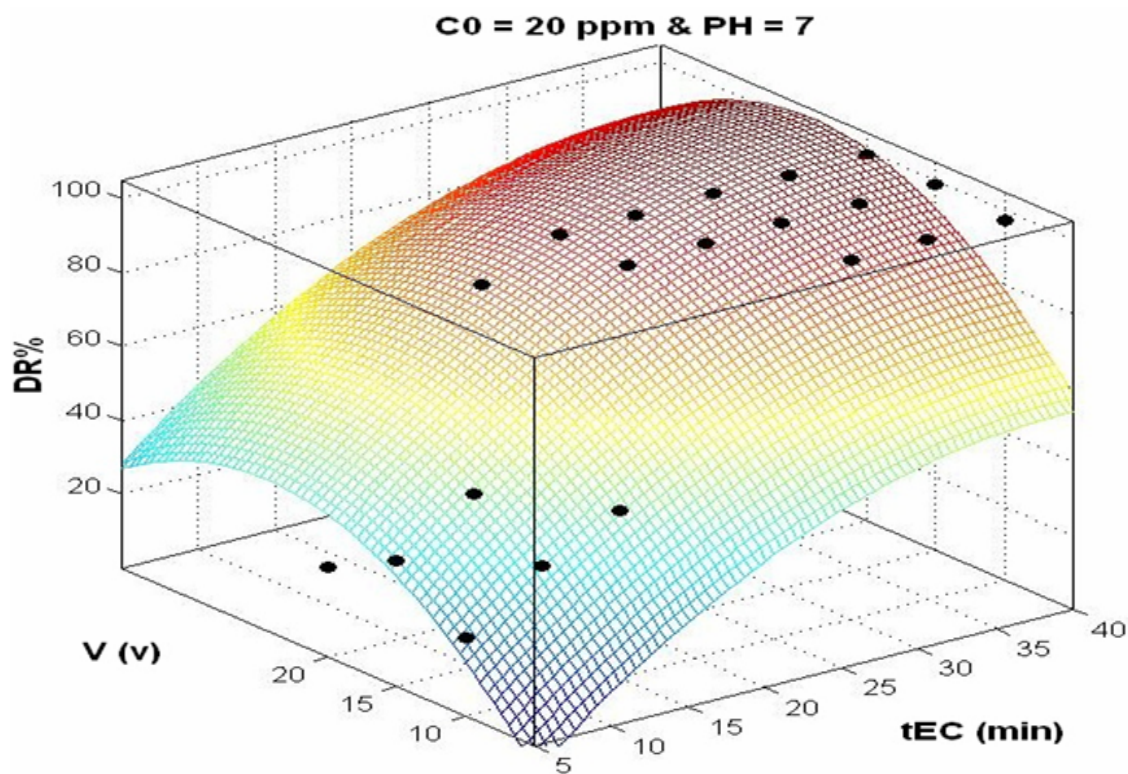| dataset		ANN	MLR
Train	Q_{ext}^2	1.00	0.79
	RMSE	0.75	14.3
Validation	Q_{ext}^2	0.98	
	RMSE	4.26	
Test	Q_{ext}^2	0.93	0.79
	RMSE	8.00	13.7

Fig. 7:   Plots of the MLR predicted values (colored surface) versus experimental DR% values (black dots) for $C_0 = 20$ (mg/L) and $pH_0 = 7$.
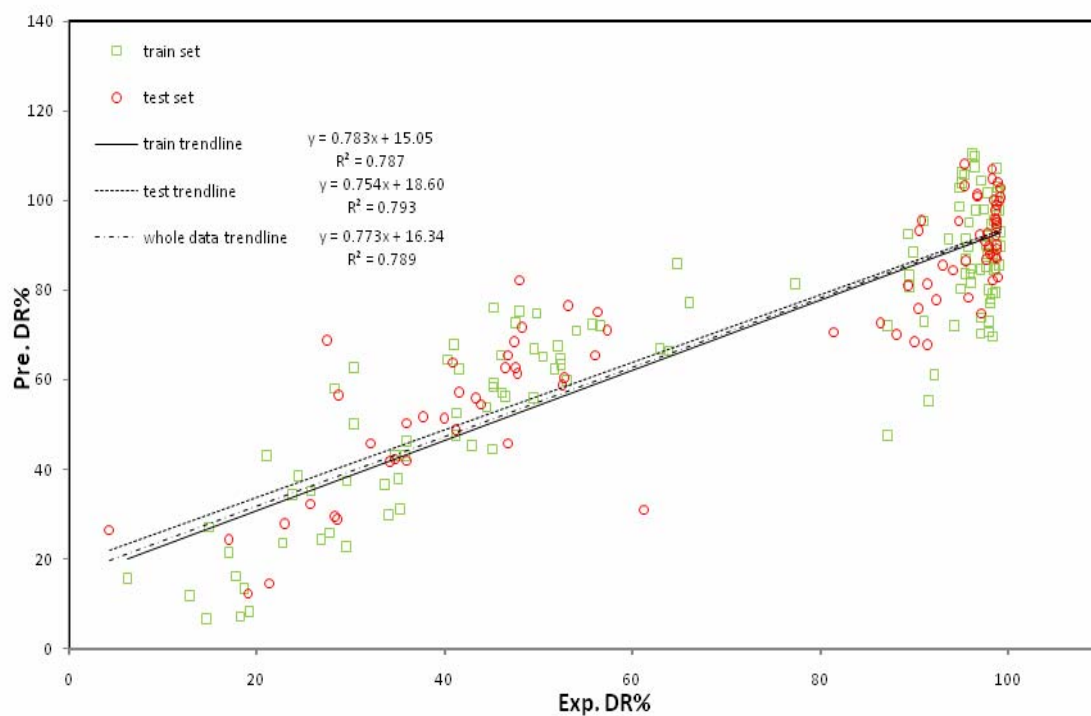

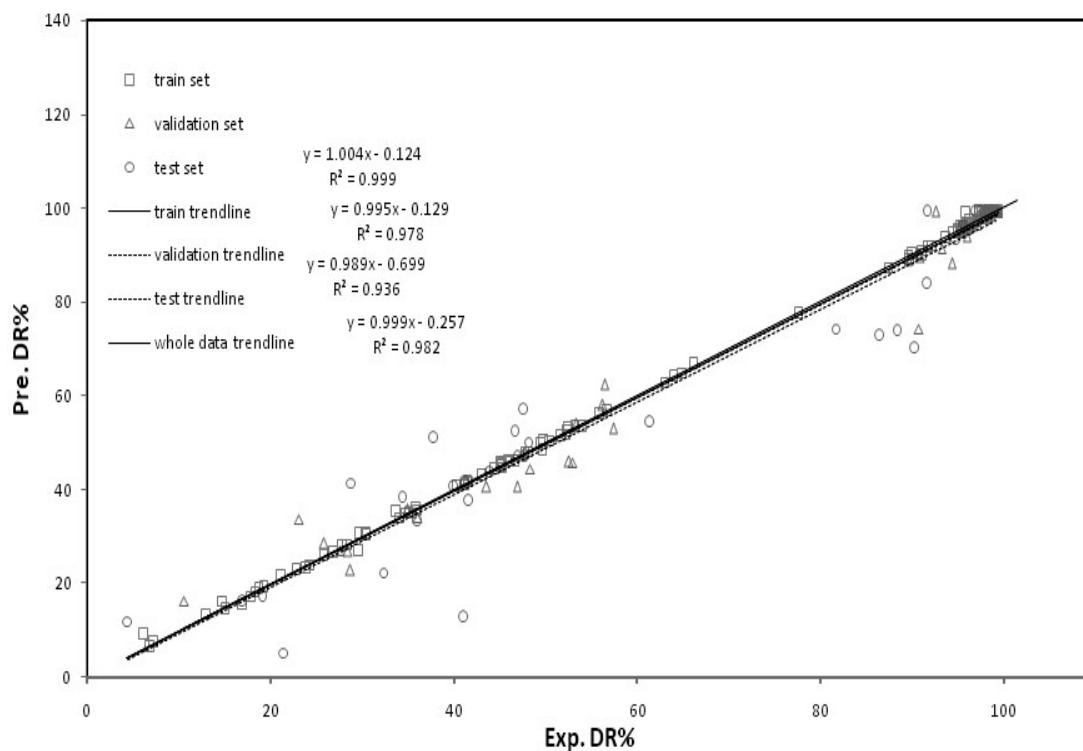Fig. 8:   The plots of predicted versus experimental DR% for MLR model.

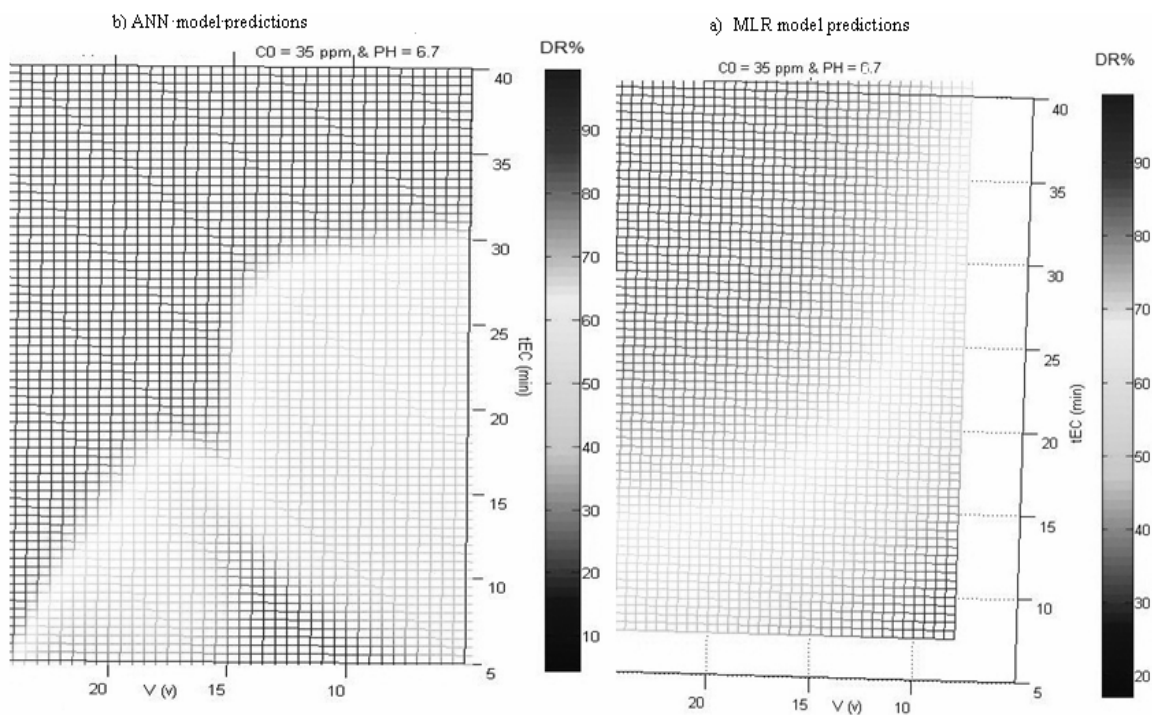Fig. 9:   The plots of predicted DR% versus experimental DR% for ANN model.

Fig. 10: Prediction of DR% for experimental rang of V_{EC} and t_{EC} in new sample with $pH_0 = 6.7$ and $C_0 = 35$ (mg/L) For a) MLR (right) and b) ANN model (left).

Further Statistical Evaluation of Models

Cross Validation

To avoid uncertainties related to select a single external test set, a more severe 216 (Leave-one-out), 5 (leave 43-44 out) and 3 (leave 72 out) - fold cross validation (CV) was used to verify the models predictability. In (n)-fold CV, the entire dataset is randomly split into n approximately equal size subsets. The model will then be trained and tested n times. Each time, one of the n subsets is used as the test set and the others (n-1) are put together to form a training set. The advantage of n-fold CV is that it is not important how the data are divided. Every data point appears in a test set only once, and in a training set (n-1) times. The overall accuracy of the constructed model is then just the simple average of the n individual accuracy measurements [38].

The Q^2_{cv} defined as a simple average of the n individual Q^2_{ext} in the 216, 5 and 3 fold cross validation. Q^2_{CV} of ANN model is 1, 0.78 and 0.75, while this value for MLR model is 0.77, 0.78 and 0.73. Based on presented Q^2 definition, these results clearly proved the logical predictability of both models .

Diversity Test

The diversity involves defining a diverse subset so that researchers can scan only a subset of the huge database each time. In this study, diversity analysis was performed for the data set to make sure that composition of the training or test sets can represent those of the whole dataset [39, 40].

A database has been considered of n experimental conditions generated from m highly correlated independent variables. Each condition X_i is represented as a vector:

$X_i = (x_{i1}, x_{i2,} x_{i3,} …,x_{im})^T$ for experimental condition with i = 1, 2, n.

Where x_{ij} denotes the value of independent variable j belongs to the condition X_i. The collective database X is represented by an n × m matrix X:

$X = (X_1, X_2, X_3, …,X_n)^T;$

Here the superscript T denotes the vector/matrix transpose. Distance score for two different experimental conditions X_1 and X_2 can be measured by the Euclidean; the mean distances of one sample to remaining ones were computed as follow:

$$d_{12} = \|X_1 - X_2\| = \sqrt{\sum_{k=1}^{m}(x_{1k} - x_{2k})^2} \qquad (4)$$

Distance normalized based on the condition independent variables:

$$\overline{d_l} = \frac{\sum_{i=1}^{n} d_{1i}}{n-1} \qquad (5)$$

Afterward the mean distances of all experimental conditions were normalized within an interval of 0-1. The closer to 1 the distance is, the more diverse from each other the compounds are. For the data sets, the normalized mean distances of experimental conditions vs. experimental DR% are shown in Fig. 11 for ANN datasets. It illustrates the diversity of experimental condition in the training and test validation sets. The training set with a broad representation of the input space was adequate to guarantee the model's stability and the diversity of test set can prove the predictive quality of the model.

Energy Consumption

To evaluate the economic feasibility of EC, the energy consumption was calculated at the mentioned optimum condition in graphical prediction of optimum condition section as following [8]:

$$\text{Energy consumption}(kwh/kg) = \frac{V_{EC} I_{EC} t_{EC}}{1000m} \quad (6)$$

Where V_{EC} is the applied voltage (Volt), I_{EC} is the average current of electrolysis (Ampere), t_{EC} is the electrolysis time (hour) and m is the weight of removed dye (kg). Weight of removed dye obtains by following equation:

$$m = 10^{-6}(C_0 - C)V \qquad (7)$$

Where V is the volume of dye solution (mg/L) and C_0 and C are initial and final dye concentrations (mg/L). It obtained 2.75 $\left(\frac{kwh}{kg}\right)$ for DR% 97 at the optimum condition. The optimum energy consumption of this quantity reported for Acid Green dye by El-Ashtoukhy *et.al* [8].
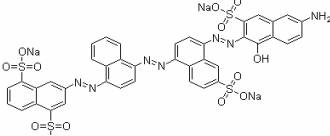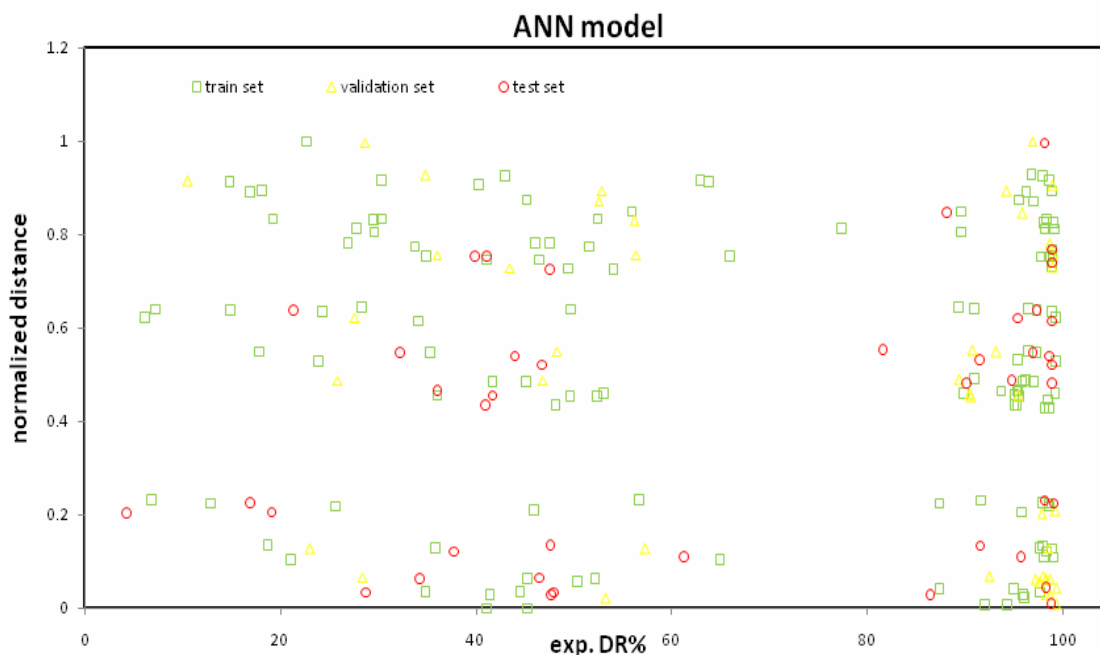
Fig. 11: The normalized mean distances of conditions vs. experimental DR% for ANN model inputs.

Table-3: The chemical properties of DB71.

Chemical Name	Direct Blue 71
Molecular Formula	$C_{40}H_{23}N_7Na_4O_{13}S_4$
CB Number	CB7141269
Molecular Structure	
Molecular Weight	1029.86
CAS Number	4399-55-7
EINECS	224-531-4
λ_{max}[1]	522 nm
[1] The maximum absorption wavelength	

[1] The maximum absorption wavelength.

Experimental

Materials and Chemical Analysis

DB71 dye purchased from (AlvandSabet, Iran). The chemical structure and some characteristics of this dye are shown in Table-3. Dye solution prepared by dissolving the dye in distilled water. pH_0 of the solution measured and adjusted by NaOH (1N) and H_2SO_4 (1N) (Merck, Germany). The dye concentration was determined by calibration curve method using a PG T80+ spectrophotometer in the UV-VIS range (200-800 nm) at the λ_{max}. The λ_{max} of the solution was obtained in each experimental condition to prevent matrix effects. After EC progress, The DR% calculated for samples by equation 8:

$$DR\% = (1- C/C_0)\times100 \qquad (8)$$

Where C_0 and C are dye concentrations (mg/L) before and after EC, respectively.

The EC system consisted of a glass (12cm*12cm*21cm (h)) Rectangular Cubic reactor, 400 rpm mixer, DC power supply (the high stability-reliability and low noise DC Adjustable Power Supply RXN-303D-II, Zhaoxin Electronic Tech. Co.) and two aluminum electrodes. lab-scale batch experimental setup of EC unit is shown in Fig. 12. The cathode and anode consist of sheets of 4cm*5cm*0.1cm dimension and the immersed surface area of each electrode was 40cm[2]. They were placed vertically and dipped in 1.5 L aqueous dye solutions. The distance between electrodes fixed at 1cm. A digital ammeter and voltmeter incorporated in the power supply applied to electrolysis current (I_{EC}) and V_{EC} monitoring during EC.

27 experiments were done in three levels of three desired parameters, C_0, V_{EC} and PH_0. In each run, 1.5 (L) dye solution was decanted into the electrolytic cell. Voltage adjusted desired value and electrolysis started. Each time, a 10 (ml) sample was extracted at same position of EC vessels in eight levels of t_{EC}, 5, 10, 15, 20, 25, 30, 35 and 40 min. using 10 (ml) pipettes. Each sample centrifuged for

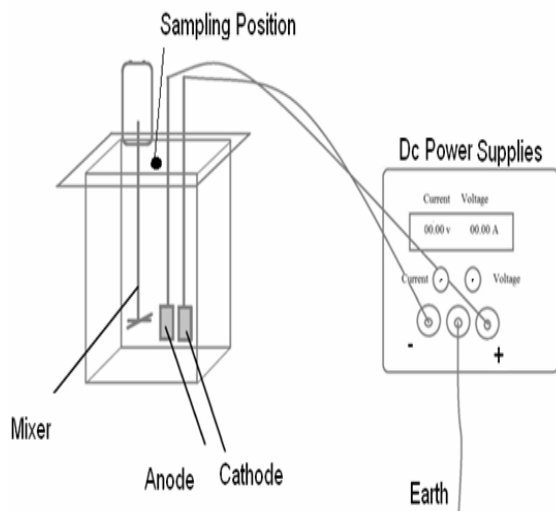10 min. in 3000 rpm. The DR% was investigated for decanted solution.

Fig. 12:　The lab-scale batch experimental setup of EC unit.

Methodology of Modeling

DR% results collected according to the experiment plan. Multiple linear regressions (MLR) and Artificial neural network (ANN) methods used to modeling EC [7, 27]. The 216 DR% together with correspond experimental condition used as a data set. The four operational parameters considered as independent variables and inputs of models whilst the DR% was dependent variable. Data set was randomly divided into three parts. The training set was used to adjust the parameters of the models, validation to overtrain prevent and testing set used to evaluate its prediction ability [41, 42]. In order to obtain a more reliable model, the parameters that affect the performance of ANN models were optimized. selection of optimal number of hidden layers, number of hidden layer neurons, initial weight, initial bias, data sets and subsets and learning rate value for ANN was performed by systemically varying their values and types in the training step [43]. All calculations carried out on a Pentium IV PC with Intel(R) core (TM) i7 2.8 GHz processor.

After the ANN model established, stepwise multiple linear regression (SMLR) method used to develop linear model based on the same ANN subsets except the test and validation sets that merged to use as an external test set. The quadratic interactions of independent variables have been considered to improve the MLR model efficiency. The more effective inputs and interactions selected using SMLR algorithm [27-29]

In the following, the consistency of the models was revealed by tests quantified with predictive Q^2. The Q^2 values measure the quality of the predictions of the held out cases exactly in the same way as R^2 does with the cases included in the modeling phase. But Q^2 is always lower and may be even negative if the predictions are worse than if we just use the average value of the response. The Q^2 value should be at least 0.3-0.4 in order to assess whether the model has statistically significant prediction ability or not [44]. The Q^2 values of the models are calculated by Equation 9.

$$Q^2 = 1 - \frac{\sum_{i=1}^{N}\left(DR\%_{exp}^{i} - DR\%_{Pre}^{i}\right)^2}{\sum_{i=1}^{N}\left(DR\%_{exp}^{i} - DR\%_{exp}^{mean}\right)^2} \quad (9)$$

Here $DR\%_{exp}$ and $DR\%_{pre}$ are the experimental and the predicted DR%, respectively. $DR\%_{exp}^{mean}$ is the average of experimental DR% for training set. Another validation analysis of the comparison of ANN with other conventional methods is RMSE (Root-Mean-Square Error) as an indicator of reliability or accuracy of the models. RMSE is computed based on the data that fit the model, and that all misfits in the data are merely a reflection of the stochastic nature of the model [44]. RMSE values of the models are calculated by Equation 10.

$$RMSE = \left[\frac{\sum_{i=1}^{N}\left(DR\%_{exp}^{i} - DR\%_{Pre}^{i}\right)^2}{N}\right]^{1/2} \quad (10)$$

Conclusion

Dye removal efficiency of solutions containing DB71 measured during EC. The effects of operational parameters of EC such as V_{EC}, pH_0, t_{EC} and C_0 were studied. The experimental results proved that EC is an effective technique for treatment of dye solutions containing DB71 and the DR% influenced by all these parameters. The effect of each operating parameter presented and studied by numerical modeling method. The ANN and MLR have been successfully used to modeling EC. By applying models to predict the test set, Q_{ext}^2 and RMSE obtained 0.79 and 13.7 for MLR and 0.93 and 8.01 for ANN. Finally, further experiments and data treatments such as new experimental condition tests, graphically selected optimum condition, diversity test, cross validation and energy consumption have

been successfully applied to the model in order to achieve more validity and to clarify other aspects of EC.

References

1. S. Papic, N. Koprivanac and A. L. Bozic, *Coloration Technology*, **116**, 352 (2000).
2. E. Rosales, M. Pazos and M. Sanroman, *Desalination*, (2011).
3. S. Bilgi and C. Demir, *Dyes and pigments*, **66**, 69 (2005).
4. H. Kusic, D. Juretic, N. Koprivanac, V. Marin and A. L. Bozic, *Journal of hazardous materials*, (2010).
5. H. Ma, M. Wang, R. Yang, W. Wang, J. Zhao, Z. Shen and S. Yao, *Chemosphere*, **68**, 1098 (2007).
6. N. Daneshvar, A. Oladegaragoze and N. Djafarzadeh, *Journal of hazardous materials*, **129**, 116 (2006).
7. N. Daneshvar, A. Khataee and N. Djafarzadeh, *Journal of hazardous materials*, **137**, 1788 (2006).
8. E. El-Ashtoukhy and N. Amin, *Journal of hazardous materials*, **179**, 113 (2010).
9. B. Merzouk, B. Gourich, A. Sekki, K. Madani, C. Vial and M. Barkaoui, *Chemical Engineering Journal*, **149**, 207 (2009).
10. M. Kobya, M. Bayramoglu and M. Eyvaz, *Journal of hazardous materials*, **148**, 311 (2007).
11. K. Yetilmezsoy, F. Ilhan, Z. Sapci-Zengin, S. Sakar and M. T. Gonullu, *Journal of hazardous materials*, **162**, 120 (2009).
12. M. Y. A. Mollah, R. Schennach, J. R. Parga and D. L. Cocke, *Journal of hazardous materials*, **84**, 29 (2001).
13. M. Y. Mollah, S. R. Pathak, P. K. Patil, M. Vayuvegula, T. S. Agrawal, J. A. Gomes, M. Kesmez and D. L. Cocke, *Journal of Hazardous Material*, **109**, 165 (2004).
14. M. Kobya, O. T. Can and M. Bayramoglu, *Journal of hazardous materials*, **100**, 163 (2003).
15. S. Irdemez, N. Demircioglu and Y. S. Yildiz, *Journal of hazardous materials*, **137**, 1231 (2006).
16. M. Kobya and S. Delipinar, *Journal of hazardous materials*, **154**, 1133 (2008).
17. M. F. Pouet and A. Grasmick, *Water Science and Technology*, **31**, 275 (1995).
18. S. H. Lin, C. T. Shyu and M. C. Sun, *Water Research*, **32**, 1059 (1998).
19. M. Kobya, H. Hiz, E. Senturk, C. Aydiner and E. Demirbas, *Desalination*, **190**, 201 (2006).
20. R. Renk, *View Record in Scopus| Cited By in Scopus* (28), 205
21. Y. Deng and J. D. Englehardt, *Waste Management*, **27**, 380 (2007).
22. H. K. Hansen, P. Nunez, D. Raboy, I. Schippacasse and R. Grandon, *Electrochimica Acta*, **52**, 3464 (2007).
23. X. Xu, X. Zeng, X. Lu, Y. Chen and H. Sun, *Industrial Water and Wastewater*, **1**, (2003).
24. C. Phalakornkule, P. Sukkasem and C. Mutchimsattha, *International Journal of Hydrogen Energy*, (2010).
25. S. Aber, A. Amani-Ghadim and V. Mirzajani, *Journal of Hazardous Materials*, **171**, 484 (2009).
26. D. Salari, A. Niaei, A. Khataee and M. Zarei, *Journal of Electroanalytical Chemistry*, **629**, 117 (2009).
27. M. S. Bhatti, D. Kapoor, R. K. Kalia, A. S. Reddy and A. K. Thukral, *Desalination*, (2011).
28. M. Nourouzi, T. Chuah and T. Choong, *Water science and technology: a journal of the International Association on Water Pollution Research*, **63**, 985 (2011).
29. A. A. Murugan, T. Ramamurthy, B. Subramanian, C. S. Kannan and M. Ganesan, *International Journal of Chemical Reactor Engineering*, **7**, 83 (2009).
30. A. Maleki, A. H. Mahvi, R. Ebrahimi and Y. Zandsalimi, *Korean Journal of Chemical Engineering*, 1 (2010).
31. R. Rezaie, A. Maleki, M. Shirzad Siboni, M. Rahimi and M. Mohammadi, *Scientific Journal of Kurdistan University of Medical Sciences*, **16**, 38 (2011).
32. M. Samarghandi, M. Shirzad Siboni, A. Maleki, S. J. Jafari and F. Nazemi, *Jouenal of Mazandaran University Medical Science*, **21**, 44 (2011).
33. A. Aleboyeh, N. Daneshvar and M. Kasiri, *Chemical Engineering and Processing: Process Intensification*, **47**, 827 (2008).
34. W. L. Chou, C. T. Wang and S. Y. Chang, *Journal of hazardous materials*, **168**, 1200 (2009).
35. M. S. Bhatti, A. S. Reddy, R. K. Kalia and A. K. Thukral, *Desalination*, (2010).
36. M. Tir and N. Moulai-Mostefa, *Journal of hazardous materials*, **158**, 107 (2008).
37. M. S. Bhatti, A. S. Reddy and A. K. Thukral, *Journal of Hazardous Materials*, **172**, 839 (2009).
38. A. Afantitis, G. Melagraki, H. Sarimveis, P. A. Koutentis, J. Markopoulos and O. Igglessi-Markopoulou, *Polymer*, **47**, 3240 (2006).

39. F. Luan, H. Liu, Y. Gao, Q. Li, X. Zhang and Y. Guo, *Journal of Colloid and Interface Science*, **336**, 773 (2009).

40. F. Luan, X. Zhang, H. Zhang, R. Zhang, M. Liu, Z. Hu and B. Fan, *Computational Materials Science*, **37**, 454 (2006).

41. M. A. Yurdusev, A. A. KumanlIoglu, Y. AbalI and M. S. Zeybek, *Construction and Building Materials*, **23**, 1871 (2009).

42. F. Ruggieri, A. A. D. Archivio, G. Carlucci and P. Mazzeo, *Journal of Chromatography* A, **1076**, 163 (2005).

43. R. Aghav, S. Kumar and S. Mukherjee, *Journal of Hazardous Materials*, (2011).

44. E. Buyukbingol, A. Sisman, M. Akyildiz, F. N. Alparslan, and A. Adejare , *Bioorganic and medicinal chemistry*, **15**, 4265 (2007).